

PACS:541,183:547:211:539,104

## OPTICAL PROPERTIES OF THE SURFACE OF RADIATION-THERMALLY OXIDIZED ALUMINUM AND BERYLLIUM

N.N. Gadzhieva

*Institute of Radiation Problems of ANAS*

[nushaba6@mail.ru](mailto:nushaba6@mail.ru)

**Abstract:** The optical properties of the surface of radiation-thermally oxidized aluminum and beryllium have been studied. Dispersion curves of effective permittivity's  $\epsilon_1(\nu)$  and  $\epsilon_2(\nu)$  are obtained. A comparative variance analysis (DA) was performed as a function of the absorbed dose of  $\gamma$ -irradiation. It was found that, depending on the absorbed dose of  $\gamma$ -irradiation, the maxima of the dispersion curves for an optical transverse phonon (TO) are mixed in the direction of high frequencies. The observed displacements are explained by the formation of oxide nanostructures on the surface of oxidized aluminum and beryllium. Optical parameters are determined - the damping frequency  $\nu_\tau$  and the plasma frequency  $\nu_p$  of the initial and radiation-thermally oxidized Al and Be within the Drude model.

**Key words:** aluminum and beryllium, optical properties, radiation-thermally oxidized, permittivity, damping and plasma frequency

### 1. Introduction

The surface layer of metals is in a special physico-chemical state. It is largely saturated with structural defects (vacancies, dislocations, impurities) and its properties differ from the bulk properties [1-5]. Therefore, the special state of the near-surface layers can influence the kinetics of various processes, including diffusion, adsorption, and radiolysis of water molecules. Contact and interaction of water with the surface of metals leads to their change and is accompanied by the formation of an oxide nanolayer. At the same time, a Me-MeO heterosystem is formed on the surface, which plays a decisive role in radiation-stimulated water processes on the surface of metals. The study of the initial stage of formation of surface oxide nanolayers is of fundamental importance for solving the problems of surface passivation and predetermines the course of the process of radiation corrosion [4,6-7]. Oxidation of metals, formation of oxide nanostructures on their surface are confirmed by the results of studies carried out using complex methods, including optical, spectroscopic, luminescent, electrophysical and microscopic methods. The dynamics of formation of oxide nanostructures is also accompanied by a change in surface properties, including optical properties. Therefore, it is interesting to study the optical properties of the surfaces of radiation-thermally oxidized aluminum and beryllium and to perform a comparative dispersion analysis of the reflection spectra as a function of the absorbed dose of  $\gamma$ -irradiation (or the contact time of aluminum and beryllium with water).

### 2. Experimental part

Plates of aluminum and beryllium with dimensions of  $20 \times 10 \times 2 \text{ mm}^3$  were investigated as objects. The plates of AD-00 grade aluminum were obtained by stage-by-stage pressing of cylindrical Al granules with a diameter of 3 and a height of 6 mm by means of a special mold designed for optical studies. [6]. The polished beryllium plates are made of an ingot Be [8].

To eliminate impurity contamination, the samples were treated with solvents (ethyl alcohol, acetone) and washed with distilled water. Samples were pre-dried at room temperature

in argon. For dehydroxylation of the surface and complete purification from organic contaminants, the samples were placed in quartz cells and additional heat treatment was carried out at 673 K in a vacuum of  $P = 10^{-6}$  Pa for 6 hours. Adsorbate was unsaturated vapors of bidistilled water from which foreign gases were removed by repeated freezing in a trap with liquid nitrogen with subsequent evacuation. Adsorption of  $H_2O$  was studied by the method described in [9, 10].

Radiation-thermal oxidation in Al (Be) / ads. $H_2O$  heterosystems was carried out at a temperature of  $T = 673K$ . The samples were irradiated on an isotope  $^{60}Co$  source with a dose rate  $d\Phi_\gamma / dt = 1.03 \text{ Gy} \cdot \text{sec}^{-1}$ . The absorbed dose, determined by the ferrosulfate dosimeter, varied within the  $\Phi_\gamma = 0.5\text{-}120 \text{ kGy}$  [11].

The reflection spectra of the initial and radiation-thermally oxidized samples of aluminum and beryllium were obtained at incidence angles  $\varphi = 88^\circ$  by the method described in [12].

The thickness of the oxide films was from 8 to 450 and 6 to 120 nm for Al and Be, respectively. The small thicknesses of oxide films were estimated by the Strohmeier formula [13] with respect to X-ray photoelectron spectra, and relatively large thicknesses were determined by gravimetric method.

### 3. The discussion of the results

Radiation-thermal processes of oxidation of aluminum and beryllium in contact with water were monitored by IR reflection-absorption spectra (IRRAS) in the frequency range 1200 - 650  $\text{cm}^{-1}$ . Figure 1 shows the changes in the absorption bands of stretching vibrations of Al-O and Be-O bonds as a function of the contact time of aluminum (Fig. 1a) and beryllium with water (Fig. 1b) with radiation-thermal oxidation ( $T = 673K$ ) Al and Be; from  $\tau = 10$  min (curve 1) to 18 hours (curve 2). As can be seen from Figs. 1a and 1b, with increasing contact time, the intensities of absorption bands of Al-O bonds ( $\nu = 950 \text{ cm}^{-1}$ ) and Be-O ( $\nu = 1100 \text{ cm}^{-1}$ ) are increased and their half-widths are broadened by  $\sim 2$  and 1.5 times, respectively. In this case, the oxide nanolayer thicknesses increase in 45 (Al) and 20 times (Be), and oxide nanostructures are formed on the surface of these metals [14, 15].

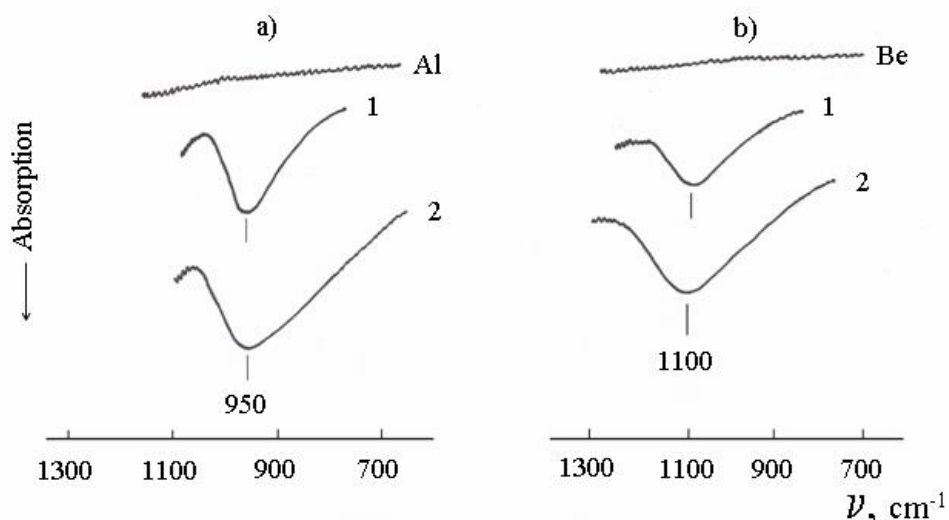


Fig.1. Changes in the absorption bands of stretching vibrations of Al-O and Be-O bonds as a function of the contact time of aluminum (Fig. 1a) and beryllium with water (Fig. 1b) with radiation-thermal oxidation ( $T = 673K$ ) of Al and Be; from  $\tau = 10$  min (curve 1) to 18 hours (curve 2)

Based on the reflection spectra, the frequency dependences of the permittivity of oxide nanolayers are obtained. As an example, the frequency dependences of the effective dielectric permittivity of natural oxide layers (solid curve) and oxide layers obtained by radiation-thermal oxidation at  $T = 673\text{K}$  on the surface of aluminum and beryllium (dashed curve) are given in the Fig. 2a and 2b illustrations. The frequency dependences are obtained for both  $\epsilon_1$  and  $\epsilon_2$ . As can be seen from the figures, the maxima of the dispersion curves for the optical transverse phonon (TO), depending on the thickness of the oxide layers, shift toward higher frequencies. The values of these displacements for heterosystems (Be-BeO) and (Al- $\text{Al}_2\text{O}_3$ ) are different and, along with other parameters, also depend on the dose of  $\gamma$ -irradiation.

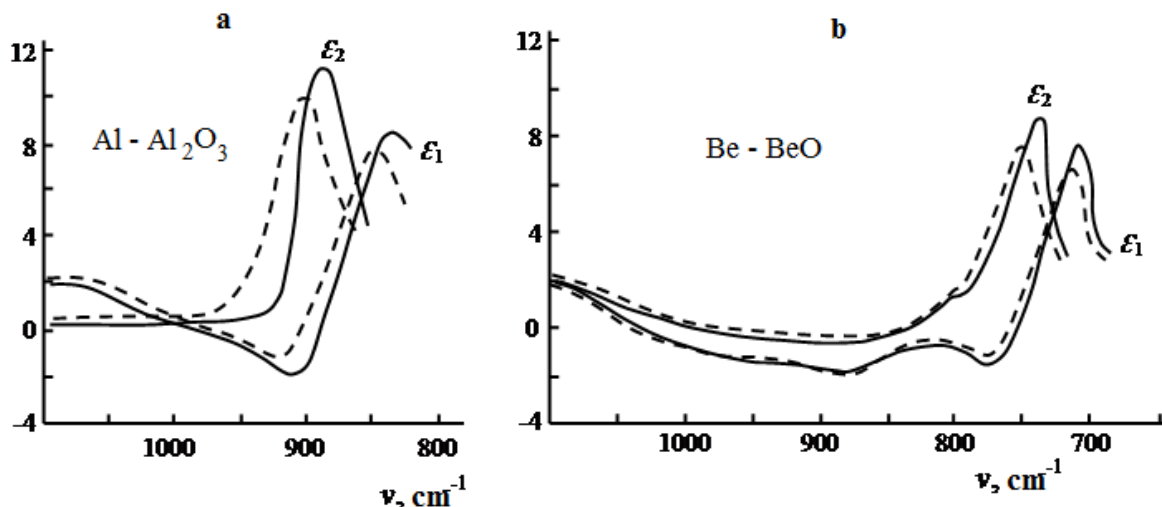


Fig.2. Effective dielectric permittivity's of the initial (solid line) and radiation-thermally oxidized at  $T = 673\text{K}$  (dashed line) of aluminum (a) and beryllium (b).

Figure 3 shows the changes in the difference values of the maximum position for TO of the Me-O bond vibration as a function of the dose of  $\gamma$ -irradiation in the radiation-thermal oxidation of Al (a) and Be (b).

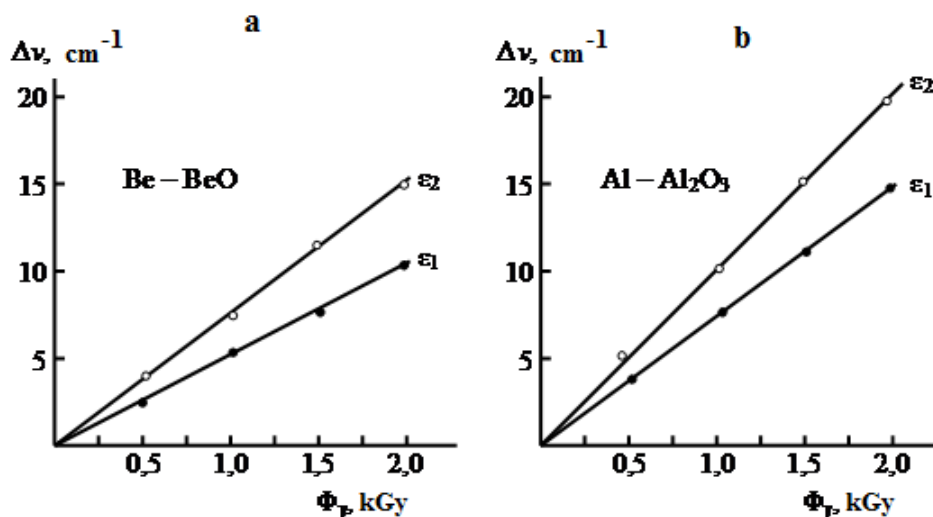


Fig.3. Changes in the difference values of the maximum position for TO of the Me-O bond vibration as a function of the dose of  $\gamma$ -irradiation in the radiation-thermal oxidation of Al (a) and Be (b)

As can be seen from the figures, the dose dependences are linear and differ in the rate of change. The rates of change, determined from the slope for the case of the heterosystem (Al-Al<sub>2</sub>O<sub>3</sub>), are ~1.4 times higher than the rate of change of the heterosystem (Be-BeO). The observed effect is apparently due to the difference in the relief and their defectiveness of the formed surface oxide nanostructures of aluminum and beryllium, which is confirmed by AGM measurements [15].

In [16], the optical parameters of a number of inert metals, including Be in the IR region, were studied and determined. It is shown that the frequency dependence of the optical parameters  $\varepsilon_1(\nu)$ ,  $\varepsilon_2(\nu)$  is well described by the Drude model [17]. It is of interest to study the optical properties and to determine the optical parameters of the initial and oxidized metallic Al and Be within the framework of the Drude model. Analogously to [16], dispersion curves  $\varepsilon_1(\nu)$ ,  $\varepsilon_2(\nu)$  were obtained. Taking IR spectroscopy into account, the frequencies are given in units of cm<sup>-1</sup>.

It is known that the complex dielectric function  $\varepsilon_c$  and the complex refractive index  $n_c$  is defined as

$$\varepsilon_c \equiv \varepsilon_1 + i\varepsilon_2 \equiv n_c^2 \equiv (n + ik)^2 \quad (1)$$

According to the Drude model, the dielectric function is described by

$$\varepsilon_c = \varepsilon_\infty - \frac{\nu_p^2}{\nu^2 + i\nu\nu_\tau} \quad (2)$$

where the values of  $\nu$ ,  $\nu_p$  and  $\nu_\tau$  are presented in cm<sup>-1</sup>. The real and imaginary parts are represented in the form

$$\varepsilon_1 = \varepsilon_\infty - \frac{\nu_p^2}{\nu^2 + \nu_\tau^2} \quad (3)$$

$$\varepsilon_2 = \frac{\nu_p^2 \nu_\tau}{\nu^3 + \nu\nu_\tau^2} \quad (4)$$

In these equations, the plasma frequency is

$$\nu_p(\text{cm}^{-1}) = \frac{1}{2\pi c} \left( \frac{4\pi N e^2}{m^* \varepsilon_\infty} \right)^{\frac{1}{2}} \quad (5)$$

where - N density of free electrons, e-electron charge, m\* - effective mass of electrons,  $\varepsilon_\infty$  - high-frequency dielectric constant. The damping frequency (the effective frequency of collisions of electrons in a metal)  $\nu_\tau$  is described,

$$\nu_\tau(\text{cm}^{-1}) = \frac{1}{2\pi c\tau} \quad (6)$$

where  $\tau$  is the electron lifetime in seconds, and c is the speed of light. It should be noted that for low frequencies

$$\varepsilon_1(0) \rightarrow -\left(\frac{\nu_p}{\nu_\tau}\right)^2 \quad (7)$$

d<sub>c</sub> conductivity  $\sigma_0$  in units of cm<sup>-1</sup> through  $\nu_p$  and  $\tau$  is defined as

$$\sigma_0 = \frac{\nu_p^2}{4\pi\nu\tau} \quad (8)$$

This dependence of d<sub>c</sub>, taking into account the resistance  $\rho_0$ , can be described in the form

$$\sigma_0(\text{CM}^{-1}) = \frac{1}{[2\pi c\rho_0(\text{s})]} = \frac{9 \cdot 10^{11}}{[2\pi c\rho_0(\Omega\text{CM})]} \quad (9)$$

According to the Drude model [17], the surface impedance is expressed as

$$Z(\nu) \equiv R(\nu) + iX(\nu) = \frac{4\pi}{c} (1 + i) \left( \frac{\nu\nu_\tau}{2\nu_p^2} \right)^{\frac{1}{2}} \left( 1 + i \frac{\nu}{\nu_\tau} \right)^{\frac{1}{2}} \quad (10)$$

Wherein

$$R(\nu) = \frac{4\pi}{c} \left( \frac{\nu\nu_\tau}{2\nu_p^2} \right)^{\frac{1}{2}} \left[ -\frac{\nu}{\nu_\tau} + \left( 1 + \frac{\nu^2}{\nu_\tau^2} \right)^{\frac{1}{2}} \right]^{\frac{1}{2}} \quad (11)$$

All data on n and k are changed and are given through  $\varepsilon_1$  and  $\varepsilon_2$ .

$$\nu_\tau = \frac{\nu\varepsilon_2}{1-\varepsilon_1} \quad (12)$$

This formula allows us to determine  $\nu_\tau$ , with the chosen frequency using the data  $\varepsilon_1$  and  $\varepsilon_2$ .

$\nu_p$  is determined from the expression (13)

$$\nu_p^2 = (1 - \varepsilon_1)(\nu^2 + \nu_\tau^2) \quad (13)$$

Using formulas 12 and 13, the values of the damping frequency (the effective frequency of collisions of electrons in the metal) and the plasma frequency  $\nu_p$  were determined at the chosen frequencies. The obtained values of these parameters are given in the table.

Table

Layer/metal, d, nm	$\nu_{LO}, \text{cm}^{-1}$	$\nu_{TO}, \text{cm}^{-1}$	$\nu_\tau, \text{cm}^{-1}$	$\nu_p, \text{cm}^{-1}$
Al <sub>2</sub> O <sub>3</sub> /Al (8 nm)	950	630	1800	59000
BeO/Be (6nm)	1100	720	510	12000
Al <sub>2</sub> O <sub>3</sub> /Al (450 nm)	950	630	1785	59200
BeO/Be (120nm)	1100	720	480	11750

It can be seen from the table that the values of the optical parameters  $\nu_\tau$  and  $\nu_p$  vary insignificantly, depending on the thickness of the oxide nanolayers. This indicates that radiation-resistant oxide nanostructures are formed on the surface of aluminum and beryllium in the region of the absorbed dose  $\Phi_\gamma = 0.5-120$  kGy at the temperature  $T = 673$  K.

#### 4. Conclusion

The optical properties of the surface of radiation-thermally oxidized aluminum and beryllium at a temperature  $T = 673$  K and under the action of  $\gamma$ -radiation are studied. Dispersion curves of effective permittivity's  $\varepsilon_1(\nu)$  and  $\varepsilon_2(\nu)$  are obtained. A comparative variance analysis (DA) was performed as a function of the absorbed dose of  $\gamma$ -irradiation. It was found that, depending on the absorbed dose of  $\gamma$ -irradiation, the maxima of the dispersion curves for an optical transverse phonon (TO) are mixed in the direction of high frequencies. The observed displacements are explained by the formation of oxide nanostructures on the surface of oxidized aluminum and beryllium. In the framework of the Drude model, the values of the optical parameters are determined: the damping frequency  $\nu_\tau$  and the plasma frequency  $\nu_p$  of the initial and radiation-thermally oxidized Al and Be.

#### References

1. Gerasimov V.V. Corrosion of reactor materials. M.: Atomizdat, 1980. 185p.
2. Konobeevsky S.T. The effect of irradiation on materials: Introduction to Radiation Material Science. M.: Atomizdat, 1980. 401p.
3. Sedov V.M., Nechaev A.F., Petrik I.G. et al. Radiation chemistry of coolants of nuclear installations: Interphase processes. L.: LTI them. Lensoveta, 1987, 58 p.
4. Platonov P.A., Tursunov I.E., Levit V.I. The influence of microstructural inhomogeneities and gas impurities on the physico-chemical properties of stainless steels // Problems of atomic science and technology. Ser.: Physics of Radiation Damage and Radiation Material Science. 1987, 2(40), p.65.
5. Kuznetsov A.M. Adsorption of water on metal surfaces // Soros' educational journal. 2000, v.6, №5, p.45.
6. Gadzhieva N.N. Oxidation and accumulation of  $H_2$  in the aluminum water system under the radiation-thermal action // Journal of Applied Spectroscopy. 2005, №4, v.72, p.471.
7. Gadzhieva N.N. Regularities of Radiation Oxidation of the Surface of Aluminum in Contact with Water // Physics and Chemistry of Materials Processing. 2010, №3, p.34.
8. Gadzhieva N.N., Garibov A.A., Ismailov Sh.S., Nurmamedova F.N. The electrophysical properties of the surface of radiation: Thermal oxidized beryllium in water medium // International Journal of Materials Science and Applications. 2014, v.3, №6-1, p.16.
9. Gadzhieva N.N., Nurmamedova F.N. Radiation oxidation of beryllium in water // Journal of Physical Chemistry. 2012, v.86, №9, p.1.
10. Gadzhieva N.N., Garibov A.A., Ismailov Sh.S. Investigation of the radiation oxidation of aluminum in the aluminum-water system by the methods of electrical conductivity and infrared spectroscopy // Problems of atomic science and technology. Ser. Physics of Radiation Damage and Radiation Material Science. 2007, №6, p.36.
11. Pikaev A.K. Modern radiation chemistry: Radiolysis of gases and liquids. M.: Nauka, 1986, p.5.
12. Gadzhieva N.N. IR spectroscopic study of radiation-stimulated adsorption of n-hexane on the beryllium surface // Optics and Spectroscopy. 2017, v.123, №1, p.22
13. Strohmeier B.R. An ESCA method for determining the oxide thickness on aluminum alloys // Surf. Interf. Anal. 1990, v.15, p.51.
14. Gadzhieva N.N., Nurmamedova F.N. Oxidation and accumulation of molecular hydrogen in beryllium water system upon radiation – thermal treatment // Protection of metals and physical chemistry of surface. 2012, v.48, №4, p.419.

15. Gadzhieva N.N, Garibov A.A, Nurmamedova F.N, Ismailov Sh.S. Microscopic examination of the surface of radiation-thermally oxidized beryllium// Problems of atomic science and technology. 2012, №5, v.81, p.21.
16. Greenler R.G. Reflection method for obtaining the infrared spectrum of a thin layer on a metal surface //J.Chem.Phys.1969, v.50, №5, p.1963.
17. P. Drude, Theory of Optics .Longmans, Green, NewYork, 1922.

## ОПТИЧЕСКИЕ СВОЙСТВА ПОВЕРХНОСТИ РАДИАЦИОННО-ТЕРМИЧЕСКИ ОКИСЛЕННОГО АЛЮМИНИЯ И БЕРИЛЛИЯ

**Н.Н. Гаджиева**

**Резюме:** Изучены оптические свойства поверхности радиационно-термически окисленных алюминия и бериллия. Получены дисперсионные кривые эффективных диэлектрических проницаемостей  $\epsilon_1(\nu)$  и  $\epsilon_2(\nu)$ . Проведен сравнительный дисперсионный анализ (ДА) в зависимости от поглощенной дозы  $\gamma$ -облучения. Выявлено, что в зависимости от поглощенной дозы  $\gamma$ -облучения максимумы дисперсионных кривых для оптического поперечного фона (ТО) смещаются в сторону высоких частот. Наблюдаемые смещения объяснены формированием оксидных наноструктур на поверхности окисленных алюминия и бериллия. Определены значения оптических параметров - частоты затухания  $\nu_t$  и плазменной частоты  $\nu_p$  исходных и радиационно-термически окисленных Al и Be в рамках модели Друде.

**Ключевые слова:** алюминий и бериллий, оптические свойства, радиационно-термическое окисление, частота затухания и плазменная частота.

## RADIASIYA-TERMİK OKSIDLƏŞMİŞ ALUMINIUM VƏ BERYLLIUM SƏTHİNİN OPTİK XASSƏLƏRİ

**N.N. Hacıyeva**

**Xülasə:** Təqdim edilmiş işdə radiasiya-termik oksidləşmiş aluminium və beryllium səthinin optik xassələri öyrənilmişdir. Effektiv dielektrik nüfuzluqlarının  $\epsilon_1(\nu)$  və  $\epsilon_2(\nu)$  dispersiya əyriləri alınmışdır. Gamma şüalanmanın udulma dozasından asılı olaraq müqayisəli dispersiya analizləri (DA) aparılmışdır. Müəyyən edilmişdir ki,  $\gamma$ -şüalanmanın udulma dozasından asılı olaraq optik eninə fononun (TO) dispersiya əyrilərinin maksimumları yüksək tezlik tərəfə sürüşürlər. Müşahidə edilən sürüşmələr alüminium və berilliumun səhində oksid nano-quruluşların yaranması ilə izah olunur. İkinci və radiasiya-termik oksidləşmiş Al və Be nümunələrin optik parametrlərinin – sönmə  $\nu_t$  və plazma  $\nu_p$  tezliklərinin qiymətləri Drude modeli çərçivəsində təyin edilmişdir.

**Açar sözlər:** alüminium və berillium, optik xassələr, radiasiya-termik oksidləşmə, nüfuzluq, sönmə və plazma tezliyi